FFI RAPPORT

EVALUATION OF CLAWPACK WITH GRAVITY AND MULTIPLE PHASES FOR USE IN MARINE TECHNOLOGY

GLATTETRE Geir Thomas

FFI/RAPPORT-2000/01060

FFIBM/410501/170

Approved
Kjeller 24 February 2000

Bjarne Haugstad
Director of Research

EVALUATION OF CLAWPACK WITH GRAVITY AND MULTIPLE PHASES FOR USE IN MARINE TECHNOLOGY

GLATTETRE Geir Thomas

FFI/RAPPORT-2000/01060

FORSVARETS FORSKNINGSINSTITUTT
Norwegian Defence Research Establishment
P O Box 25, N-2027 Kjeller, Norway

FORSVARETS FORSKNINGSINSTITUTT (FFI)
Norwegian Defence Research Establishment

P O BOX 25
2027 KJELLER, NORWAY

UNCLASSIFIED

SECURITY CLASSIFICATION OF THIS PAGE
(when data entered)

REPORT DOCUMENTATION PAGE

1) PUBL/REPORT NUMBER	2) SECURITY CLASSIFICATION	3) NUMBER OF PAGES
FFI/RAPPORT-2000/01060	UNCLASSIFIED	48
1a) PROJECT REFERENCE	2a) DECLASSIFICATION/DOWNGRADING SCHEDULE	
FFIBM/410501/170	-	

4) TITLE

EVALUATION OF CLAWPACK WITH GRAVITY AND MULTIPLE PHASES FOR USE IN MARINE TECHNOLOGY

5) NAMES OF AUTHOR(S) IN FULL (surname first)

GLATTETRE Geir Thomas

6) DISTRIBUTION STATEMENT

Approved for public release. Distribution unlimited. (Offentlig tilgjengelig)

7) INDEXING TERMS

IN ENGLISH:	IN NORWEGIAN:
a) Computational fluid dynamics	a) Numerisk væske simulering
b) Conservation laws	b) Konserverings lover
c) Godunov methods	c) Godunov metoder
d) Gravity	d) Gravitasjon
e) Boundary conditions	e) Grensebetingelser

THESAURUS REFERENCE:

8) ABSTRACT

This thesis concerns the use of the program package CLAWPACK (Conservation LAWs PACKage) in problems related to marine technology. Problems investigated are vortex shedding, multiple phases and gravity. This thesis includes mathematical theory of the governing equations and principles of CLAWPACK. Further, it contains a discussion on boundary conditions, several ways of handling gravity and validation tests with results and discussions.

9) DATE	AUTHORIZED BY This page only	POSITION
24 February 2000	Bjarne Haugstad	Director of Research

ISBN 82-464-0410-5

UNCLASSIFIED

SECURITY CLASSIFICATION OF THIS PAGE
(when data entered)

CONTENTS

2 HYPERBOLIC CONSERVATION LAWS AND NUMERICAL METHODS

In order to understand the CLAWPACK code the user must have some knowledge of hyperbolic conservation laws and numerical methods. The greater part of the time spent on this thesis was used to obtain this knowledge. This chapter is presented for completeness of the thesis and is based on [20] and [23].

2.1 Hyperbolic Conservation Laws

Hyperbolic conservation laws are mathematical statements of physical conservation properties. They are widely used in modeling fluid dynamical phenomena. Conservation laws are partial differential equations with an especially simple form. A one-dimensional system of m conservation laws may be written as

$$q_t + f(q)_x = 0, \tag{2.1}$$

where $q = q(x,t) \in \mathbb{R}^m$ is the conserved quantity, and f is the flux function. Subscripts denote partial differentiation.

To see how conservation laws arise from physical principles, first comes a derivation of the equation for conservation of mass in a one-dimensional gas dynamics problem. The problem concerns flow in a tube where properties of the gas such as density and velocity are assumed to be constant across each cross section of the tube. Let x represent the distance along the tube and let $\rho(x,t)$ be the density of the gas at point x and time t. This density is defined in such a way that the total amount of gas in any given section between the fixed boundaries x_1 and x_2 is given by the integral of the density:

$$\text{mass in } [x_1, x_2] \text{ at time } t = \int_{x_1}^{x_2} \rho(x,t)\, dx. \tag{2.2}$$

If we assume that the walls of the tube are impermeable and that mass is neither created nor destroyed, then the mass in this one section can change only because of gas flowing across the boundaries x_1 and x_2. Now let $u(x,t)$ be the velocity of the gas at time t. Then the rate of flow, or *flux* of gas past this boundary is given by

$$\text{mass flux at } (x,t) = \rho(x,t)u(x,t). \tag{2.3}$$

The rate of change of mass in $[x_1, x_2]$ is given by the difference in fluxes at x_1 and x_2:

$$\frac{d}{dt}\int_{x_1}^{x_2} \rho(x,t)\, dx = \rho(x_1,t)u(x_1,t) - \rho(x_2,t)u(x_2,t). \tag{2.4}$$

A main feature of the conservation laws is their ability to develop discontinuous solutions. An example is shock produced in front of aircrafts moving at supersonic speed. Even when the initial conditions are smooth, the solution will in general develop discontinuities in finite time.

The discontinuities represent a challenge due to non-uniqueness in the solution and discontinuities in its derivatives. A mathematical maneuver performed to ease the smoothness constraints of the solution is the weak solution.

A natural way to define a generalized solution of the in-viscid equation that does not require differentiability is to go back to the integral form of the conservation law, and say that $q(x,t)$ is a generalized solution if (2.5) is satisfied for all x_1, x_2, t_1, t_2.

There is another approach that results in a different integral formulation that is often more convenient to work with. This is a mathematical technique that can be applied more generally to rewrite a differential equation in a form were less smoothness is required to define a "solution". The basic idea is to take the PDE, multiply it by a smooth *test function*, integrate it one or more times over some domain, and then use integration by parts to move derivatives off the function q and onto the smooth test function. The result is an equation involving fewer derivatives on q, and hence requiring less smoothness. In our case we will use test functions $\phi \in C_0^1(\mathbb{R} \times \mathbb{R})$. C_0^1 is the space of functions that are continuously differentiable with compact support. If we multiply $q_t + f_x = 0$ by $\phi(x,t)$ and then integrate over space and time, we obtain

$$\int_0^\infty \int_{-\infty}^{+\infty} [\phi q_t + \phi f(q)_x]\, dx\, dt = 0. \tag{2.11}$$

Now integrate by parts, yielding

$$\int_0^\infty \int_{-\infty}^{+\infty} [\phi_t q + \phi_x f(q)]\, dx\, dt = -\int_{-\infty}^{+\infty} \phi(x,0) q(x,0)\, dx. \tag{2.12}$$

Note that nearly all the boundary terms which normally arise through integration by parts drop out due to the requirement that ϕ has compact support, and hence vanishes at infinity. The remaining boundary term brings in the initial condition of the PDE, which must still play a role in the weak formulation. The function $q(x,t)$ is called a weak solution of the conservation law if (2.12) holds for all functions $\phi \in C_0^1(\mathbb{R} \times \mathbb{R})$ [23].

Due to the conservation properties, there has to be a connection between the velocity of the discontinuity s, the left state q_l, and the right state q_r at the discontinuity. From the definition of a weak solution, we obtain

$$s(q_l - q_r) = f(q_l) - f(q_r). \tag{2.13}$$

This relation is named the *Rankine-Hugoniot* (RH) condition.

2.2 Numerical methods

The presence of discontinuities complicates numerical solution of conservation laws. First order accurate schemes produce an excessive amount of dissipation near shocks and discontinuities. The result is that these features are smeared out over several grid cells causing loss in resolution. The truncation error is dominated by second order terms, and acts as an artificial viscosity.

Second order accurate schemes have truncation errors dominated by third order terms. This results in spurious oscillations near the discontinuities giving the schemes a dispersive character. For non-linear problems, this may result in severe oscillations causing a breakdown in the computations.

There are two main approaches used to overcome these problems. These are *shock fitting* (or *shock tracking*) and *shock capturing*.

In the first, used on steady state problems, the discontinuities are handled separately from the rest of the solution. The discontinuities are treated as internal boundaries using the Rankine-Hugoniot relations (2.13) as boundary conditions, while the rest of the solution is treated with standard finite difference methods. The special treatment of the discontinuities produces accurate representations of the shocks, but the position of the shock waves and how they interact, must to some extent be known in advance. On time dependent problems one needs to keep track of the movement of the discontinuities, and this complicates the schemes. Further, there is difficulty involved in accuracy and convergence assessment.

In shock capturing, the same algorithm is used on the entire solution, which simplifies the scheme. The schemes uses second order accurate solution methods as a basis for solving the hyperbolic conservation laws. The schemes are however constructed to reduce the spurious oscillations associated with second order accurate methods near oscillations. The discontinuities are smeared out over a small number of grid cells.

The first important paper on shock capturing was published in 1950 by von Neumann and Richtmeyer [34]. They studied gas dynamics using second order accurate schemes. In real fluids, the discontinuities are not infinitely sharp, but extend over a thin layer due to viscosity and diffusive properties. In order to reduce non-physical oscillations in their solutions they added small amounts of *artificial viscosity*. The goal was to keep the representation of the shock sharp, while minimizing oscillations. Later Lapidus [21] formulated this approach in a two step procedure. The solution were computed in a first step using a second order accurate scheme, and in a second step he solved a diffusion problem.

The disadvantage of the above mentioned shock capturing approaches is their problem dependency. The amount of artificial viscosity needed is highly problem dependent, meaning the methods must be tuned to each individual problem.

In 1960, Lax and Wendroff [22] introduced the conservation form of a finite difference

the method may be formulated as a conservative scheme, and the time step constraint may be relaxed to the more liberal $s\Delta t \leq \Delta x$. This scheme is first order accurate. In addition, the complexity in computing the Riemann solution caused this scheme to be only slowly adapted. Instead approaches like the artificial viscosity were used for many years.

Based on Glimm's famous theorem on existence of weak solutions for systems of conservation laws [13], Chorin [4] constructed another Riemann solution based computational scheme. Instead of using the average of the Riemann solution as the numerical approximation at the next time level, the value at a random point inside the cell is used. Due to this, the scheme is named the *Random Choice Method*, RCM. The result is a scheme with excellent approximation of discontinuities, which makes this schemes especially attractive on combustion problems were this is of major importance.

Two decades after the initial work by Godunov, van Leer resurrected his upwind approach, and developed a second order extension [33]. He considered the Euler equations and achieved second order accuracy by constructing linear approximations to the solution within each cell, in contrast to the constant approximation used by Godunov. The slopes in this piecewise linear approximation are chosen so that no new extrema are introduced and so that conservation is ensured. This piecewise linear approximation gives rise to more complicated initial value problems at the interfaces than the Riemann problem. However, it is possible to approximate this problem by solving a Riemann problem with modified left and right states. This algorithm was named the MUSCL scheme, an acronym for Monotonic Upstream-centered Scheme for Conservation Laws. In this original work by van Leer, the scheme consisted of a Lagrangian step, in which the Riemann problem was solved, followed by an Eulerian step.

Colella reformulated this scheme into a single Eulerian step, in addition to simplifying the approximation of the Riemann solution [6]. Other approaches in the same direction are based on using polynomials of higher degree than one in the reconstruction. In the *Piecewise Parabolic Method* (PPM), Colella and Woodward [8] apply quadratic approximations within each cell resulting in third order spatial accuracy. Even higher order polynomials are used in the *Essentially Non-Oscillatory* (ENO) schemes by Harten and Osher [19].

Harten introduced the concept of *Total Variation Diminishing* (TVD) schemes [18]. The total variation of a *scalar* numerical solution q_i^n is defined as

$$TV(q^n) = \sum_i |q_{i+1}^n - q_i^n|. \tag{2.19}$$

Note that this definition may be viewed as a measure on the "oscillations" of the solution. Total variation diminishing means that $TV(q^{n+1}) \leq TV(q^n)$. The TVD concept implies that q^{n+1} cannot amplify extrema in q^n nor create new ones. If it did, the total variation would increase. In the paper Harten derived simple conditions for a scheme to be TVD. An implication of the concept of total variation is connected to the question of convergence. The set of functions with uniformly bounded total variation is compact, hence any infinite

property of the Roe solver is that $A(q_r - q_l) = f(q_r) - f(q_l)$, which is necessary for obtaining a conservative scheme. A consequence of this property is that if the exact solution consists of a single shock, or is dominated by a shock, this will also be the case for the approximative solution. The Riemann problem of a linear system with m components consists of m discontinuities. In cases were the exact solution involves rarefaction waves, this may lead to entropy violating solutions. Hence, an entropy condition is needed. A theorem due to Harten and Lax states that if the conservation law has an entropy function, then it is in principle possible to construct a Roe solver [16].

Up to this point it has been focused on one dimensional applications. However, the majority of problems of practical interest are multi dimensional. There is a considerable activity going on in diciplines related to this topic, for example grid generation. The underlying grid may be used in characterizing multi dimensional methods. In what follows I will only consider Cartesian grids and rectangular computational grid cells.

A commonly used approach on such grids is to apply *dimensional splitting*. The numerical approximation is defined by performing sweeps along one dimensional strips of cells. In the simplest dimensional splitting scheme, the numerical solution at the next time level, i.e. q^{n+1} is defined as follows for the two dimensional problem $q_t + f(q)_x + g(q)_y = 0$. Based on q^n the one dimensional problem $q_t + f(q)_x = 0$ is solved for a time step Δt for every row in the grid. The intermediate values obtained are used as initial condition when $q_t + g(q)_y = 0$ is solved for another time step Δt for every column, and q^{n+1} is defined as the solution obtained. This splitting scheme is formally first order accurate in Δt. The slightly more complicated *Strange splitting* is second order accurate. Strange splitting involves solving the first one dimensional conservation law equation over a half time-step, then solving the second one dimensional equation over one whole time step, and finally solving the first equation over the last half step. Crandall and Majda [10] have for the scalar case proved convergence to the unique entropy solution for both splitting schemes when the one dimensional problems are solved exactly. In a result by Teng [32], it is proved that the convergence rate for both schemes are $O(\sqrt{\Delta t})$.

Any one dimensional shock capturing scheme may be used in the splitting resulting in an easy extension to multi dimensional extension to multi dimensional problems. Remarkably good results may be obtained using this approach. Another advantage is that the stability equals the stability of the one dimensional schemes.

There are however several disadvantages with dimensional splitting. The schemes are strongly directional dependent, since "numerical" waves only propagate in the coordinate directions. The effect is that discontinuities propagating obliquely to the grid experience more smearing than the ones traveling close to the coordinate directions. In the same way, dimensional splitting schemes have trouble with keeping symmetries. Further, we have that dimensional splitting in connection with very accurate one dimensional schemes may produce unphysical waves in the vicinity of discontinuities. A well known example is the failure of the Random Choice Method when applied to multi dimensional gas dynamics [5].

As for one dimensional problems, upwind schemes constitutes an important class of

3 CLAWPACK

3.1 Governing Equations

The CLAWPACK (Conservation LAWs PACKage) is a program package for solving time-dependent hyperbolic systems in one, two and three space dimensions. Recall that in one dimension the standard non-linear conservation law is given as

$$q_t + f(q)_x = 0. \tag{3.1}$$

In this thesis, the conservation laws used will be the Euler equations which in one dimension are

$$\begin{bmatrix} \rho \\ \rho u \\ E \end{bmatrix}_t + \begin{bmatrix} \rho u \\ \rho u^2 + p \\ u(E+p) \end{bmatrix}_x = 0. \tag{3.2}$$

The Euler equations describe the flow of an in-viscid gas with no heat conduction. They may be deduced by the Navier-Stokes equations by setting viscosity and heat conductivity equal to zero.

The one dimensional Euler equations contains four unknowns in a system of three equations, so an additional relation is needed. This is done by introducing the energy equation

$$E = \frac{1}{2}\rho u^2 + \frac{p}{(\gamma - 1)} \tag{3.3}$$

This energy equation describes total energy as a sum of kinetic and internal energy. The internal energy is deduced from the equation of state for a polytropic gas with γ being the same gas constant as in (2.15).

Equation (3.2) and (3.3) may be put in the form (3.1) where

$$q(x,t) = \begin{bmatrix} \rho(x,t) \\ \rho(x,t)u(x,t) \\ E(x,t) \end{bmatrix} \equiv \begin{bmatrix} q_1 \\ q_2 \\ q_3 \end{bmatrix} \tag{3.4}$$

and

$$f(q)_x = \begin{bmatrix} \rho u \\ \rho u^2 + p \\ u(E+p) \end{bmatrix} = \begin{bmatrix} q_2 \\ q_2^2/q_1 + p(q) \\ q_2(q_3 + p(q)/q_1 \end{bmatrix}. \tag{3.5}$$

linearization in this case. Since (3.7 i) guarantees that the method behaves reasonably on an isolated discontinuity, it is only when a Riemann problem has a solution with more than one strong shock or contact discontinuity that the approximative Riemann solution will differ significantly from the true Riemann solution. In practice this happens infrequently, for example when two shocks collide.

One way to guarantee that both conditions (3.7 ii) and (3.7 iii) are satisfied is to take

$$\hat{A}(q_l, q_r) = f'(q_{ave}) \tag{3.8}$$

for some average value of q, *e.g.*, $q_{ave} = \frac{1}{2}(q_l + q_r)$. Unfortunately, this simple choice of q_{ave} will not give an $\hat{A}$ that satisfies (3.7 i) in general.

One disadvantage of Roe's linearization is that the resulting approximate solution consists only of discontinuities, with no rarefaction waves. This can lead to a violation of the entropy condition, particularly if the solution involves transsonic rarefaction. In the case of a sonic rarefaction wave, it is necessary to modify the approximate Riemann solver in order to obtain entropy satisfying solutions. There are various ways to do this and a standard method is implemented in CLAWPACK.

3.3 Godunov Methods

Recall that each cell has a constant value interpreted as a cell average. This value must be updated for each time step. The change of value equals the sum of net flux at both cell interfaces. This flux is calculated using the wave speed λ^p, from the Riemann problem together with the size of the discontinuity across the interfaces. The flux is regarded as constant over each time step.

The first order Godunov method is implemented in a form that requires a *flux-difference splitting* which is a decomposition of $f(q_r) - f(q_l)$ into a *left-going flux-difference* denoted by $\mathcal{A}^-\Delta q$, and a *right-going flux-difference* denoted $\mathcal{A}^+\Delta q$, with the property that

$$\mathcal{A}^-\Delta q + \mathcal{A}^+\Delta q = f(q_r) - f(q_l)\,. \tag{3.9}$$

For the classical Godunov method, let $q* = Q(0)$ be the value along $x/t = 0$ in the solution to the Riemann problem. Then

$$\begin{aligned} \mathcal{A}^-\Delta q &= f(q^*) - f(q_l) \\ \mathcal{A}^+\Delta q &= f(q_r) - f(q^*). \end{aligned} \tag{3.10}$$

If a wave decomposition on the form (2.17) is available, one can alternatively set

where q_i^* is the intermediate state arising in solving the Riemann problem at x_i. This numerical method is clearly in conservation form and is typically stable for Courant numbers up to 1. Equation (3.15) can be rewritten by the use of equation (3.10) as

$$\overline{q}_i = q_i - \frac{\Delta t}{\Delta x}(\mathcal{A}^+ \Delta q_i + \mathcal{A}^- \Delta q_{i+1}). \tag{3.16}$$

Here $\mathcal{A}^+ \Delta q_i$ is the right-going flux difference from solving the Riemann problem between q_{i-1} and q_i. This models the combined effect on the cell average q_i of all waves entering the cell from the left edge. Similarly, $\mathcal{A}^- \Delta q_{i+1}$ is the left going flux difference from the Riemann problem between q_i and q_{i+1}, and models the combined effect of all waves entering the cell from the right. For a system of conservation laws, (3.16) is conservative and consistent for any flux-difference splitting that satisfies (3.9). Nonconservative systems does not yield equation (3.15), but by using piecewice constant initial data, and then computing cell averages to define $\overline{q}_i$, Riemann problems can be effectively implemented in the form (3.16).

Godunov methods as described here are only first order accurate.

3.4 High Resolution Methods

First order methods will smear out the solution. This is especially true for rapid shifts in gradients and discontinuities. The result is large numerical diffusion. Second order methods will smear out less, but have a tendency to oscillate in the vincinity of rapid shifts in gradients and discontinuities leading to numerical dispersion. A high resolution method must be able to handle discontinuities satisfactory without excessive numerical diffusion or dispersion. This is accomplished by introducing a correction term to the first order Godunov method making it second order accurate, combined with a limiter to the correction term in order to minimize oscillations in the solution.

3.4.1 Second Order Corrections

In the first order Godunov method, the initial solution was approximated by piecewise constant initial data. In order to introduce a second order correction term, this approximation is refined to a piecewise linear approximation with the same cell average as before. Alternatively, the correction terms may be viewed as correction waves accompanying the first order waves described earlier.

Equation (3.16) is a first order advancement of the solution to the next time step. The method can be extended to

$$\overline{q}_i = q_i - \frac{\Delta t}{\Delta x}(\mathcal{A}^+ \Delta q_i + \mathcal{A}^- \Delta q_{i+1}) - \frac{\Delta t}{\Delta x}(\tilde{F}_{i+1} - \tilde{F}_i). \tag{3.17}$$

upwind direction; i.e., we look to the left if $\lambda_i^p > 0$ and to the right if $\lambda_i^p < 0$. In the case of the linear system (3.12) we have

$$\mathcal{W}_i^p = \alpha_i^p r^p, \tag{3.22}$$

where α_i^p is a scalar and the vector r^p is independent of i. Then we can simply apply the limiter to the scalars α_i^p, setting $\tilde{\mathcal{W}}_i^p = \tilde{\alpha}_i^p r^p$, where $\tilde{\alpha}_i^p$ is the limited wave strength. This is calculated by applying some limiter function ϕ to the ratio of this wave strength to the strength of the neighboring wave in the same family, looking in the upwind direction,

$$\tilde{\alpha}_i^p = \phi(\theta_i^p)\alpha_i^p, \tag{3.23}$$

where

$$\theta_i^p = \frac{\alpha_I^p}{\alpha_i^p} \quad \text{with } I = \begin{cases} i-1 & \text{if} \quad \lambda_i^p > 0 \\ i+1 & \text{if} \quad \lambda_i^p < 0 \end{cases} \tag{3.24}$$

The ratio of wave strengths θ_i^p is used to measure the smoothness of the solution. Where the solution is smooth, this can be expected to be near unity. Near discontinuities in the pth family, θ_i^p may be far from unity. A wide variety of limiter functions have been studied, some standard limiters used in CLAWPACK are

minmod:	$\phi(\theta) = max(0, min(1, \theta))$
superbee:	$\phi(\theta) = max(0, min(1, 2\theta), min(2, \theta))$
monotonized centered (MC):	$\phi(\theta) = max(0, min(\frac{(1+\theta)}{2}, 2, 2\theta))$.

For variable coefficient or nonlinear problems the wave $\mathcal{W}_i^p$ will not be a scalar multiple of the waves $\mathcal{W}_{i-1}^p$ or $\mathcal{W}_{i+1}^p$ from the neigboring Riemann problem, and one must determine the manner in which these vectors are going to be compared and modified in applying the limiter. For concreteness assume $\lambda_i^p > 0$ so that the pth family we compare $\mathcal{W}_i^p$ and $\mathcal{W}_{i-1}^p$. The approach used is to project the neighboring wave $\mathcal{W}_{i-1}^p$ onto the vector $\mathcal{W}_i^p$ and compare the length of this projected vector with the length of $\mathcal{W}_i^p$ itself, modifying the length of $\mathcal{W}_i^p$ as needed, but preserving its direction. This is accomplished by setting

$$\begin{aligned} \theta_i^p &= \frac{\mathcal{W}_{i-1}^p \cdot \mathcal{W}_i^p}{\mathcal{W}_i^p \cdot \mathcal{W}_i^p} \\ \tilde{\mathcal{W}}_i^p &= \phi(\theta_i^p)\mathcal{W}_i^p, \end{aligned} \tag{3.25}$$

where $\cdot$ represents inner product. Note that this reduces to (3.24) for a linear system.

$\mathcal{B}^+\mathcal{A}^*\Delta q_{ij}$ (the up going transverse fluctuation) and $\mathcal{B}^-\mathcal{A}^*\Delta q_{ij}$ (the down going transverse fluctuation).

Introducing transverse propagation has two important effects. First, it provides the cross derivatives terms q_{xy} and q_{yx} required in a second order algorithm. Once the transverse flux has been included, second order accuracy is easily achieved by including the second derivative terms in each coordinate direction (q_{xx} and q_{yy}) using the same correction that is applied in one space dimension. Second, the transverse correction terms improve the stability limit and allow full Courant number 1, relative to the maximum wave speed in any direction. For more details see [25]

4 MODIFICATIONS TO THE CLAWPACK CODE

CLAWPACK is a package of Fortran subroutines for solving time-dependent hyperbolic systems in one, two and three space dimensions. It provides a framework for user supplied or adapted subroutines used to define the problem of interest. The package supports the use of a designated subroutine for implementation of boundary conditions and likewise a subroutine for implementation of source terms using time steps of length dt or $dt/2$ (Strange splitting).

Modifications can thus be regarded as a customization of the user supplied subroutines.

4.1 Boundary Conditions

Outer boundaries limiting the computational domain may be implemented as either reflecting solid wall boundaries or open boundaries (4.1).

Boundary conditions are implemented by assigning values to two rows of ghost cells added to the outskirts of the computational domain. The values of the ghost cells are related to the values of computational cells directly inside the domain. The implementation of boundary conditions described below are not strictly conservative.

Non-reflecting boundary conditions are also known as open boundary conditions or artificial boundaries. They are used when the problem of interest is not limited by walls. Open boundaries should thus replicate infinity by letting the solution exiting the domain do so, without reflecting disturbances back into the solution. Artificial boundaries will, ofcourse, never be able to model infinity in the case of incoming flow.

In the simulations, open boundaries are implemented by assigning values to the two rows of ghost cells based on the outermost computational cells as shown in figure (4.2). The Ghost cells are given values according to

$$\rho|_{Ghost\ cell\ 1.row} = \rho|_{Ghost\ cell\ 2.row} = \rho|_{Comp.\ cell\ 1.row} \tag{4.1}$$

$$\rho u|_{Ghost\ cell\ 1.row} = \rho u|_{Ghost\ cell\ 2.row} = \rho u|_{Comp.\ cell\ 1.row}$$
$$\rho v|_{Ghost\ cell\ 1.row} = \rho v|_{Ghost\ cell\ 2.row} = \rho v|_{Comp.\ cell\ 1.row}$$
$$E|_{Ghost\ cell\ 1.row} = E|_{Ghost\ cell\ 2.row} = E|_{Comp.\ cell\ 1.row}.$$

Reflecting boundary conditions are also known as solid wall or no-cross flow boundary conditions. They are used when the problem of interest are restricted by solid walls. The exiting solution should be reflected back into the computational domain. This is done by assigning values according to (4.2) and figure (4.3).

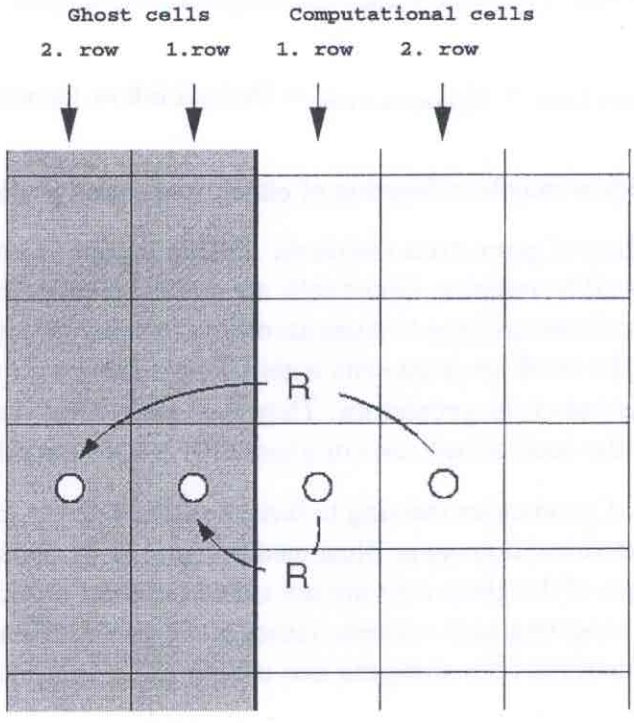

Figure 4.3: Reflecting boundary conditions.

$$\begin{aligned}
\rho|_{Ghost\ cell\ 1.row} &= \rho|_{Comp.cell\ 1.row} \\
\rho|_{Ghost\ cell2.row} &= \rho|_{Comp.cell\ 2.row} \\
\rho u|_{Ghost\ cell\ 1.row} &= -\rho u|_{Comp.\ cell\ 1.row} \\
\rho u|_{Ghost\ cell\ 2.row} &= -\rho u|_{Comp.\ cell\ 2.row} \\
\rho v|_{Ghost\ cell\ 1.row} &= \rho v|_{Comp.\ cell\ 1.row} \\
\rho v|_{Ghost\ cell\ 2.row} &= \rho v|_{Comp.\ cell\ 2.row} \\
E|_{Ghost\ cell\ 1.row} &= E|_{Comp.\ cell\ 1.row} \\
E|_{Ghost\ cell\ 2.row} &= E|_{Comp.\ cell\ 1.row}.
\end{aligned} \tag{4.2}$$

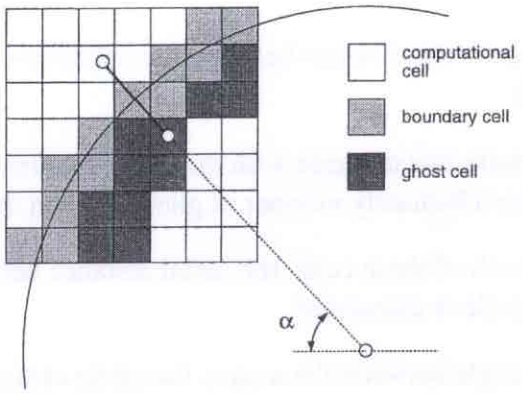

Figure 4.5: Boundary conditions of circular objects.

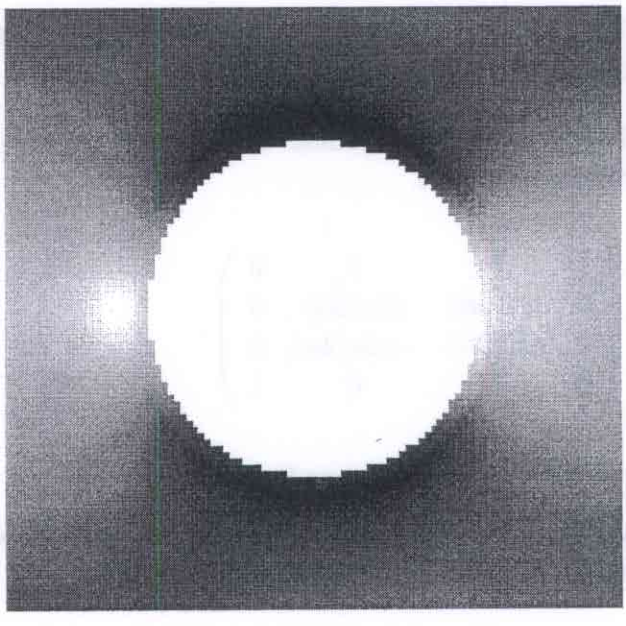

Figure 4.6: Circle modeled by the described boundary conditions. The ghost cells and the boundary is showing outside the white filling.

general form of the conservation law with source term becomes

$$q_t + f(q)_x + g(q)_y = \psi(q), \tag{4.5}$$

with ψ being the source term.

The two dimensional Euler equations including gravity will thus be

$$\begin{bmatrix} \rho \\ \rho u \\ \rho v \\ E \end{bmatrix}_t + \begin{bmatrix} \rho u \\ \rho u^2 + p \\ \rho uv \\ u(E+p) \end{bmatrix}_x + \begin{bmatrix} \rho v \\ \rho uv \\ \rho v^2 + p \\ v(E+p) \end{bmatrix}_y = \begin{bmatrix} 0 \\ 0 \\ -\rho g \\ -\rho g v \end{bmatrix} \tag{4.6}$$

where $E = \frac{1}{2}\rho(u^2 + v^2) + \frac{1}{\gamma - 1}p$ and gravity appears in the source terms. $g = 1/\gamma$.

Implementing these source terms in the CLAWPACK code can be done in various manners.

4.2.2 Time Splitting

In this work, the source terms are implemented using time splitting. Using time splitting, (4.5) is decomposed into the homogeneous conservation law (3.1), and an ordinary differential equation (ODE)

$$q_t = \psi(q). \tag{4.7}$$

In the current case, the Euler equations with gravity, the homogeneous part is equation (4.6) with the right hand side being all zeros, while the system of ODEs is

$$\begin{bmatrix} \rho \\ \rho u \\ \rho v \\ E \end{bmatrix}_t = \begin{bmatrix} 0 \\ 0 \\ -\rho g \\ -\rho g v \end{bmatrix}. \tag{4.8}$$

The calculations can thus be performed as earlier with an additional system of ODEs solved over the same time step in a separate operation.

In this work the implementation of source terms are done as follows.

At the start of each time step, boundary conditions are set using the standard boundary condition subroutine. Secondly, the Riemann solver solves the homogeneous equations as in the absence of source terms. This calculation spans the whole time step. Then, the subroutine solving the ODEs are called, solving the ODEs over the same time step

$$\rho|_{Ghost\ cell\ 2.row} = \rho|_{Comp.\ cell\ 2.row}$$
$$\rho u|_{Ghost\ cell\ 1.row} = \rho u|_{Comp.\ cell\ 1.row}$$
$$\rho u|_{Ghost\ cell\ 2.row} = \rho u|_{Comp.\ cell\ 2.row}$$
$$\rho v|_{Ghost\ cell\ 1.row} = -\rho v|_{Comp.\ cell\ 1.row}$$
$$\rho v|_{Ghost\ cell\ 2.row} = -\rho v|_{Comp.\ cell\ 2.row}$$
$$E|_{Ghost\ cell\ 1.row} = (E|_{Comp.\ cell\ 1.row} \times \gamma + \rho|_{Comp.\ cell\ 1.row} \times\ grav \times dy)/\gamma$$
$$E|_{Ghost\ cell\ 2.row} = (E|_{Comp.\ cell\ .row} \times \gamma + \rho|_{Comp.\ cell\ 1.row} \times\ grav \times 3 \times dy)/\gamma.$$

The assumption of constant density near the reflecting boundary is suspect. In problems involving flow at the boundaries, the pressure (energy) part of the solution must be handled with more care. For the simulations performed in this thesis, the boundary conditions in (4.11) are sufficient since the simulations are terminated before momentums reach the boundaries.

As for open boundaries with gravity, the vertical boundaries do not need to be modified.

Inflow conditions are implemented in the same fashion as without gravity. The only care that must be taken is that the flow parameters match the problem investigated with regard to initial conditions and pressure equilibrium.

The method of time splitting may not be suited for near steady state solutions with small perturbations. The reason for this is that the source terms are added to the steady state solution for then to be corrected by the next solution of the Riemann problem. The result of one large contribution to be cancelled by a correspondingly large correction in the Riemann solver may be inaccurate. Further, we have that limiters are applied in the solution procedure of the Riemann problem, while the solution of the ODEs stands uncorrected [28].

5 VALIDATION TESTS

5.1 Scaling

The parameters for time, length, velocity, pressure, gravity and density needs to be converted from the units used in the simulations to physical units. The basic parameters are time and length. From these parameters, one can deduce the others. Subscript 0 denote scaling factors.

As an example, we have that $t_{real} = t_{computation} \times t_0$.

As we are dealing with a compressible gas, velocity is scaled by the mach number as

$$U_0 = \frac{1}{\sqrt{\gamma}} * c, \tag{5.1}$$

left boundary. Initial conditions were set with uniform velocity except for a vertical disturbance introduced at the leeward side of the object. The vertical velocity component were the same size as the initial horisontal velocity. The simulation was terminated at simulation time 1800.

Results The simulation shows unsymmetric vortex shedding. The vortices are shed from the downwind corners of the rectangle as expected. The wake do not evolve into a stable von Karmann vortex street. The distribution of vortices behind the object seems random. The measurements at a point located 100 cells left of the right boundary (5.1) shows oscillation in vertical velocity.

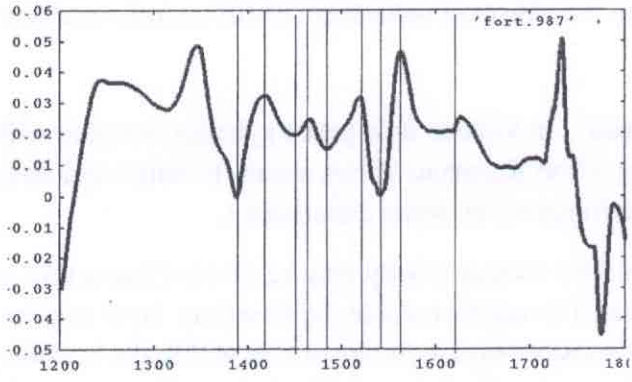

Figure 5.1: Vertical velocities as a function of time behind rectangle.

Discusion The rectangle have sharp corners defining the separation point of the flow. Thus, alternate vortex shedding from a rectangle do not involve relocation of the separation point. The phenomenon is not dependent of a accurate modelling of the boundary layer. The compressible Euler equations handles compressibility and is not limited to irrotational flow.

5.2.2 Circle

The simulation is performed on a 600×300 grid with open boundaries. The object is modelled as a circle with radius spanning 20 grid cells. Inflow is defined on the left boundary. Initial conditions were set with uniform velocity except for a vertical velocity component, of the same size as the horisontal velocity component, introduced at the windward side of the circle. The simulation was terminated at simulation time 600.

Results A vortex street is not seen, but there are varying vertical velocities behind the circle, figure (5.2).

equations are in-viscid, and therefore not capable of reproducing a boundary layer. The failure to produce a Von Karmann vortex street is thus consistent with in-viscid flow theory.

The results do however show a varying vertical velocity behind the cicle indicating the presence of such a vortex street. This needs to be investigated further. This simulation ran for approximately a week.

5.3 Two phase

Godunov methods are well suited to capture discontinuities. In order to investigate CLAWPACKs ability to handle density discontinuities, I use a test case modeling gases of two different densities with zero momentum in initial conditions. The setup is run to see wether CLAWPACK is able to "hold" the solution, or if velocities are created. Any velocities will be non physical. The density relation between the upper and lower gas is one to five, and there are 100 grid cells in vertical direction.

Results The simulation produces vertical velocities at the discontinuity. These are in the range of 10^{-15}.

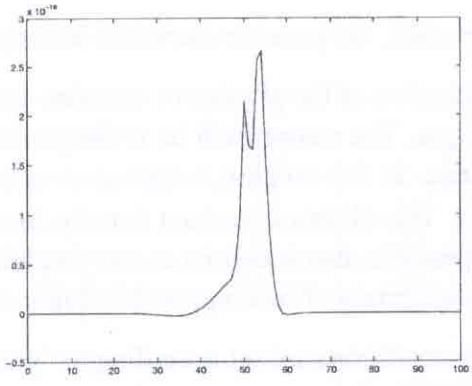

Figure 5.3: Velocities at $t = 0.5$ in two phase setup without gravity. $\rho_1 = 1$, $\rho_2 = 5$ and $p = 1$ in top. The computational domain is resolved by 100 grid cells vertically.

Discusion Vertical velocities are produced at the interface between the two gases. Since there is no diffusive term in the governing Euler equations, the velocities are clearly an error related to the scheme or round-off errors. In the construction of the approximative Roe solver, condition (3.7 i) ensures that the approximative solution is exact across the discontinuity. One can thus conclude that the errors are solely round-off errors.

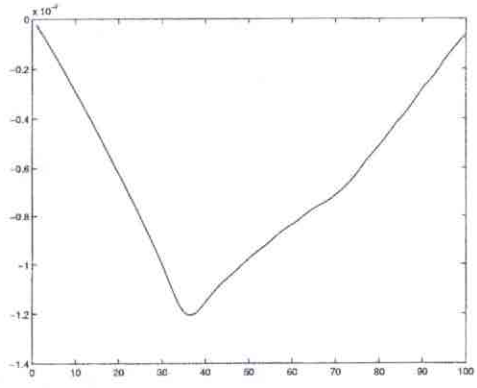

Figure 5.4: Velocities at $t = 0.5$ in setup with constant density, $\rho = 1$, $p = 1$ in top and gravity. The computational domain is resolved by 100 grid cells vertically.

5.4.2 Two Phase Hydrostatic Equilibrium

A test case is set up with two phases and hydrostatic equilibrium. A low density gas is defined on top of a heavier gas. Each of the two phases is given a hydrostatic equilibrium, with continuity of pressure across the interface of the two gases. The momentum is set to zero everywhere and boundary conditions are given as in the case of hydrostatic equilibrium.

Results Dominating velocities are introduced at the interface between the high and low density gases. The velocyties are in the range of 10^{-3}. Starting at the interface, the area of momentum spreads to the rest of the domain.

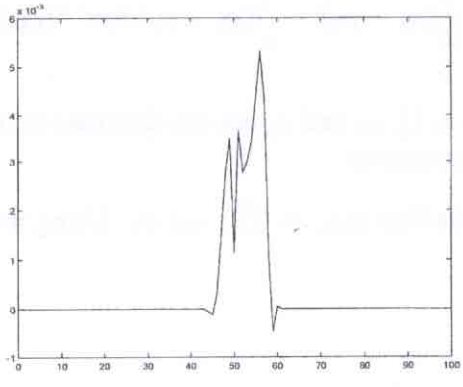

Figure 5.5: Velocities at $t = 0.05$ in two phase setup with gravity. $\rho_1 = 1$ and $\rho_2 = 5$, $p = 1$ in top. The computational domain is resolved by 100 grid cells vertically.

Discusion The model produces large momentums. Doubling the resolution does not reduce the errors. The results are clearly non-physical and the error is to large to be

6.2 Wave Modification

Gravity appears as a source term in the Euler equations. This source term may be implemented by introducing a new discontinuity with Riemann problems to be solved in the center of each grid cell. The discontinuity will be in the density and energy equations. Pressure is indirectly given by the energy equation.

The introduction of an additional discontinuity with the associated Riemann problems in every grid cell represents a vast increase in computational cost. The increase in computational cost of each time step becomes even more severe as the effective width of the grid cells is halved. The stability constraints will then lead to halving of the time steps as well.

This motivates an alternative implementation of the same principle. Instead of introducing new discontinuities in the center of each grid cell, the source terms may be implemented be modifying the left and right states of the existing Riemann problems. This implementation allows the original spatial grid and time steps to be unchanged. Further we have that no additional Riemann problems need to be solved.

The implementation of gravity through modification of left and right states in the Riemann problems ensures that perturbations are calculated by a single set of waves of size relevant to the size of the perturbation. This is a major improvement of the scheme minimizing numerical errors when it is used to solve small perturbations near steady state.

By modifying the values of the cell averages, we can incorporate the source terms in the solution of the Riemann problems. This leads to solving both the homogeneous part as well as the source term in the same procedure. Numerical errors are thereby minimized by describing perturbations directly and not by introducing large sources and correspondingly large corrections. More details can be found in [26], and [28].

The implementation of wave modification used in [28] is based on as assumption of "small" perturbations. The presented results are based on a truncated solution of the modifications implied on to states in the Riemann problems. The truncation error may be minimized by implementing an iteration procedure using the truncated solution as an initial guess.

6.3 Extraction of Perturbations

Another alternative algorithm may be deduced by subtracting the initial condition from the solution, and thus solve with regard to the remaining perturbations.

In the case of an initial pressure balance, where subscript 0 denote initial state, we get

$$\begin{aligned} \rho &= \rho_0 + \tilde{\rho} \\ p &= p_0 + \tilde{p} \end{aligned} \tag{6.3}$$

$$B(q) = \begin{bmatrix} v & 0 & \rho & 0 \\ 0 & v & 0 & 0 \\ 0 & 0 & v & 1/\rho \\ 0 & 0 & \gamma p & v \end{bmatrix}, \tag{6.11}$$

and

$$h = \begin{bmatrix} 0 \\ 0 \\ -g \\ 0 \end{bmatrix}. \tag{6.12}$$

The non-conservative formulation is used with time splitting. Only the vertical velocity component is modified, and either a standard Riemann solver or the formulation

$$A_1 = \frac{1}{2}(A(q_l) + A(q_r)) \tag{6.13}$$

may be used.

7 CONCLUSION

The CLAWPACK code was originally designed for solving problems involving shocks using conservation laws. Due to its ability to handle discontinuities, it would be interesting to see whether it can be used on problems originating in marine technology, especially handling of a free surface. Gravity and curved geometries have been implemented.

The implementation of a circle was successful. Simulations of vortex shedding shows physical behavior. Approaching the problem of a free surface, it is found that the code holds initial conditions with discontinuous density profile. Implementing gravity, the code shows satisfying results on holding a hydrostatic equilibrium with constant density. Problems arise when applying varying density.

The CLAWPACK code used with the Euler equations is not developed as a tool for solving problems involving a free surface. Further work has to be done in order to implement and verify capability to handle gravity combined with discontinuities. Suggestions to alternative algorithms for implementation of gravity are given.

[17] A. Harten and G. Zwas. Self-adjusting hybrid schemes for shock computations. *Journal of Computational Physics*, 9, 1972.

[18] E. Harten. High resolution schemes for hyperbolic conservation laws. *Journal of Computational Physics*, 49, 1983.

[19] E. Harten and S. Osher. Uniformly high-order accurate non-oscillatory schemes, i. *SIAM J. Numer. Anal.*, 24, 1987.

[20] Jan Olav Langseth. *Wave Propagation Schemes, Operator Splitting, and Front Tracking for Hyperbolic Conservation Laws*. PhD thesis, University Of Oslo, 1996.

[21] A. Lapidus. *Journal of Computational Physics*, 2, 1967.

[22] P.D. Lax and B. Wendroff. Systems of conservation laws,ii. *Comm. Pure Appl. Math.*, 13, 1960.

[23] Randall J. LeVeque. Nonlinear conservation laws and finite volume methods for astrophysical fluid flow. Lecture Notes.

[24] Randall J. LeVeque. *Numerical Methods for Conservation Laws*. Birkhäuser, 1990.

[25] Randall J. LeVeque. Wave propagation algorithms for multidimensional hyperbolic systems. *JOURNAL OF COMPUTATIONAL PHYSICS*, 131(2), March 1997.

[26] Randall J. LeVeque. Balancing source terms and flux gradients in high-resolution godunov methods: The quasi-steady wave-propagation algorithm. *Submitted to Journal of Computational Physics*, 1998.

[27] Randall J. LeVeque. *CLAWPACK User Notes*. Applied Mathematics, University of Washington, http://www.amath.washington.edu/ rjl/clawpack.html, draft edition, November 95.

[28] Randall J. LeVeque and Derek S. Bale. Wave propagation methods for conservation laws with source terms. In *Proc. 7'th Int'l Conf. on Hyperbolic Problems, z ürich,1998*.

[29] P.L. Roe. Approximate riemann solvers, parameter vectors, and difference schemes. *Journal of Computational Physics*, 43, 1981.

[30] C.W. Schulz-Rinne, J.P. Collins, and H.M. Glaz. Numerical solution of the riemann problem for two-dimensional gas dynamics. Technical report, ETH Zurich, 1992. Seminar fur Angewandte Mathematik.

[31] P.K. Sweeby. High resolution schemes using flux limiters for hyperbolic conservation laws. *SIAM J. Numer. Anal.*, 21, 1984.

[32] Z.H. Teng. On the accuracy of fractional step methods of conservation laws in two dimensions. *Journal of Numerical Mathematics*, 31, 1994.

DISTRIBUTION LIST

FFIBM **Dato:** 24 februar 2000

RAPPORTTYPE (KRYSS AV)	RAPPORT NR.	REFERANSE	RAPPORTENS DATO
X RAPP ☐ NOTAT ☐ RR	2000/01060	FFIBM/ 410501/170	24 februar 2000
RAPPORTENS BESKYTTELSESGRAD		**ANTALL EKS UTSTEDT**	**ANTALL SIDER**
UNCLASSIFIED		25	48
RAPPORTENS TITTEL		**FORFATTER(E)**	
EVALUATION OF CLAWPACK WITH GRAVITY AND MULTIPLE PHASES FOR USE IN MARINE TECHNOLOGY		GLATTETRE Geir Thomas	
FORDELING GODKJENT AV FORSKNINGSSJEF:		**FORDELING GODKJENT AV AVDELINGSSJEF:**	

EKSTERN FORDELING

ANTALL	EKS NR	TIL
1		Randall J. LeVeque University of Washington Department of Applied Mathematics Box 352420 Seattle, WA 98195-2420 USA
1		www.ffi.no

INTERN FORDELING

ANTALL	EKS NR	TIL
14		FFI-Bibl
1		Adm direktør/stabssjef
1		FFIE
1		FFISYS
1		FFIBM
1		Øyvind Andreassen, FFIBM
1		Jan Olav Langseth, FFIBM
4		Geir Thomas Glattetre, FFIBM
1		ffi-veven

FFI-K1 Retningslinjer for fordeling og forsendelse er gitt i Oraklet, Bind I, Bestemmelser om publikasjoner